

THE 4TH INTERNATIONAL CONFERENCE ON ALUMINUM ALLOYS

AS-CAST STRUCTURE AND RECRYSTALLIZATION BEHAVIOUR IN TWIN-ROLL CAST AL-MG ALLOY

B.S. Berg, V. Hansen and J. Gjønnes

Centre for Materials Research/Physics Department, University of Oslo, Gaustadalléen 21, N-0371 Oslo, Norway

Introduction

Twin roll casting (TRC) has for some time been an alternative to conventional DC casting and hot rolling. The relatively low productivity and alloy limitations has been a drawback for further exploitation. Hydro Aluminium has a pilot plant operating at the R&D Centre, Karmøy in order to evaluate the potential for improved productivity by casting at thinner gauges and higher casting speeds. The alloy investigated in this paper is AA5052 (Al-2.5%Mg), mainly used for canning material. TRC involves an increase in cooling rate during solidification compared to DC casting, and also a decrease in hot working deformation prior to cold rolling. In order to investigate the variations in microstructure across the strip, an overall optical characterization is a first step to understand the solidification. Higher resolution microscopy (SEM, TEM) is needed for a more complete picture of the solidification like element distribution and phase characterization in the cross section.

The aim of the present study is to describe the microstructural variations and development from the as-cast state through cold rolling and annealing as a function of process parameters. The observations are compared with results of computer modelling of temperature, melt flow, deformation and stresses in the process [1].

Experimental

The material is from a 2³ factorial design considering the three parameters set-back, casting speed and strip thickness, each at two levels. In addition to these 8 combinations, the strip thickness was successively reduced in 5 steps giving a total of 13 different combinations. The alloy composition and a selection of the casting parameters are summarized in Table I. The as-cast structure was analysed optically in a Reichert MeF3 microscope equipped with a Kontron Vidas25 image analysing system.

By scalping the samples along an oblique plane chosen to be approximately normal to the solidification front, we can obtain a three dimensional description of the grain structure sketched in Fig. 1. Grain volumes were measured in 1/8 thickness intervals from the surface. Cell-/dendrite arm spacings (DAS) were measured after the anodized layer had been removed by 10% H₃PO₄ at 82°C (50 sec.) [2]. Cell spacings were used to calculate the cross section cooling rates.

Table I. Alloy composition and a selection of casting parameters

Alloy:	Si	Fe	Mn	Mg	Cu	Ti	B	Zn	Cr	V			
AA5052	0.05	0.28	0.005	2.42	0.003	0.002				0.24			
	#1	#2	#3	#4	#5	#6	#7	#8	#9	#10	#11	#12	#13
Setback [mm]:	40	44	44	40	40	44	44	40	44	47	49	50	50
Thickness [mm]:	4.91	4.98	4.54	4.52	4.48	4.5	5.03	4.98	4.02	3.34	2.52	2.14	1.87
Strip speed: [m/min]:	1.32	1.32	1.02	1.02	1.32	1.32	1.02	1.02	1.56	2.1	2.94	3.94	5.04

Particle size distributions were measured in a JEOL 733 Superprobe scanning electron microscope at 10kV using a Link image analysing system. Magnification used was x2000 and AlFe particles were measured in backscatter mode.

A 5.0mm and a 1.9mm thick sheet(#7 and #13), were laboratory cold rolled to 0.5mm and annealed at 350°C/h for 3 hrs.(heating rate 100°C/h). Specimens were collected in 15 min intervals. Planar sections parallel to the surface were polished at three levels: a) at the surface, b) at 1/6 of the thickness and c) at the central part; (111) pole figures were collected with a Siemens texture camera operating according to the Schultz method. Hardness measurements were carried out in a Zwick hardness-tester.

Phase identification, crystal structure and particle compositions of primary and secondary particles were studied by transmission electron microscopy using standard foil preparation techniques and extraction of particles by a dissolution technique [3]. The microscopes used, JEOL 200CX and JEOL 2000FX, are both equipped with EDS attachments.

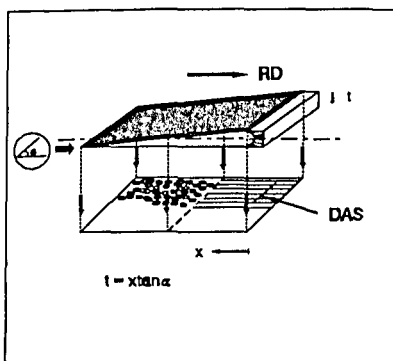


Fig.1. Scalping the samples along an oblique plane

Results

As-cast structure

The micrographs in Fig. 2 a-d show the grain and dendrite structure in the first (a,c) and last (b,d) casting referring to Table I. The microstructure of the 5mm strip (#1) is characterized by the well-known two-part grains with a dendritic head followed by a cellular tail, elongated in the casting direction. The 1.9mm strip (#13) show a much smaller, less elongated and a purely equiaxed structure. This is the typical structure for the thinnest castings, i.e. <2.6mm. The grain size, as represented by volume, Fig.3, is seen to increase from the surface towards the centre. Measurements from the surface of the castings were difficult to obtain because of the severe deformation in this area.

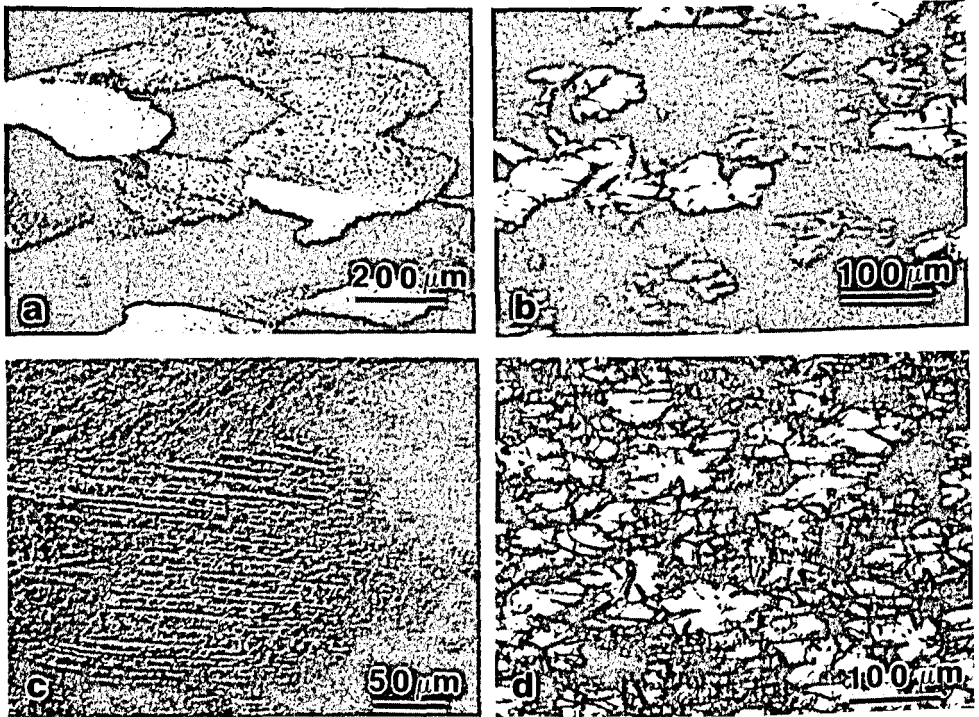


Fig.2. Optical micrographs of grain structure and dendrite structure in casting #1 a) + c), and casting #13 b) + d).

DAS measured in the cellular area of the castings #1-#10 (>2.6mm), are plotted in Fig. 4. The spacings vary from a value of approximately $4\mu\text{m}$ in the surface to $6-8\mu\text{m}$ in the centre. In the thinnest strip with equiaxed structure the dendrites are coarser; as can be seen from Fig. 4a and Fig. 2c,d. The values were more than doubled in casting #13 compared to #1 and #8.. The relation between DAS and cooling rate has been confirmed by several authors [4-7]. Using the relation proposed by Strid [7], the average cooling rate was found to be one order of magnitude lower in the thinnest as compared with the thicker strip (Fig. 4b).

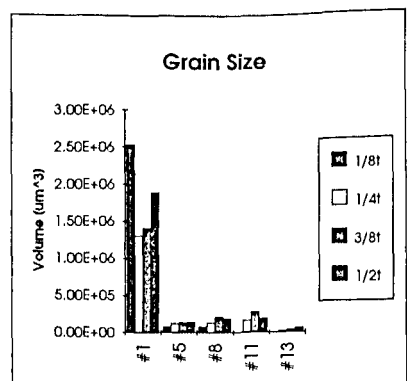


Fig. 3. Grain sizes across the strip

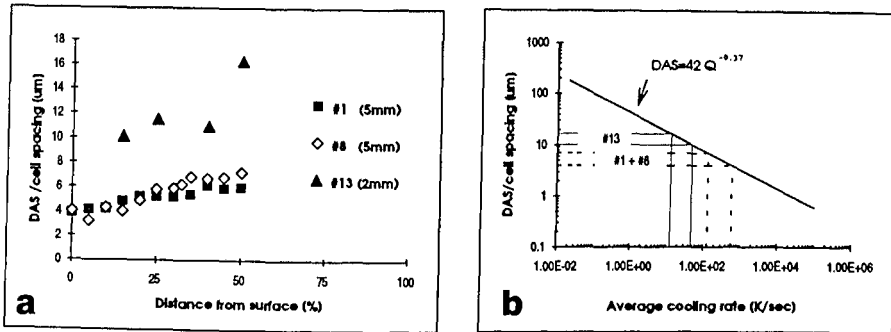


Fig.4. Cell spacings in three castings a), and correlated cooling rates b) [7].

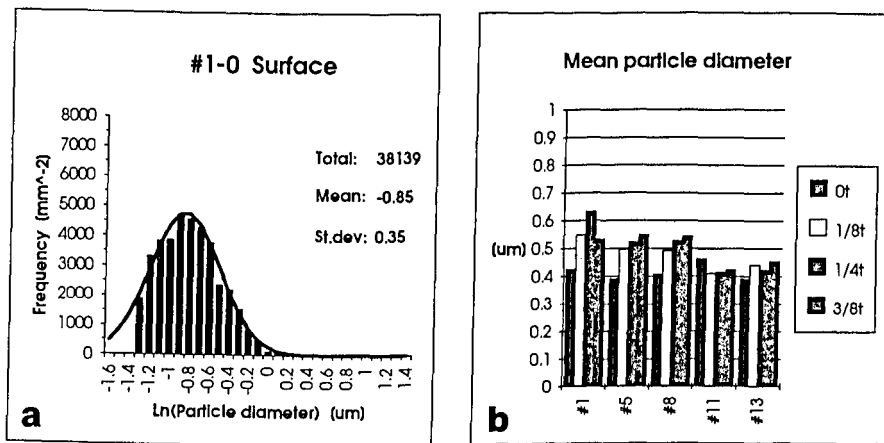


Fig.5. a) Logarithmic particle distributions in surface of casting #1, b) mean particle diameter in five different castings.

Logarithmic particle size distributions in the surface of casting #1 is shown in Fig. 5a. The mean particle sizes are found by fitting a lognormal curve to the upper part of the distribution. Particles less than $0.28\mu\text{m}$ were excluded. There are less but larger particles in the centre of the strip. The same adjustment is done for a selected number of casting in four different sections. A summary of these results is given in Fig. 5b. There is an increase in sizes and decrease in the total number of particles from the surface towards the centre.

Phase characterizations in TEM showed the metastable Al_mFe to be the most common primary phase. The unit cell is body-centred tetragonal ($a=8.84\text{\AA}$, $c=21.6\text{\AA}$) [5,8] and a possible space group $I4/mmm$ has been suggested by Skjerpe [8]. The value of m has been measured to be in the range 4.0 - 4.4 [9-11]. The monoclinic equilibrium phase Al_3Fe is found, mainly in the centre. Mg_2Si and Al_8Mg_5 is also found in the centre of the strip.

Cold rolled and annealed structure

Two strips, #7 and #13, were cold rolled to 0.5mm thickness and annealed at constant heating rate. Grain structures obtained after cold rolling and after annealing for 2.5hrs and 6.5hrs are shown in Fig. 6a-f. The deformation from the cold rolling is concentrated near the surface, as seen in Fig. 6a,d. Despite considerable difference between the strain levels recrystallization was found to start after 2.5hrs heat treatment, corresponding to a top temperature of 250°C, Fig. 6b,e.

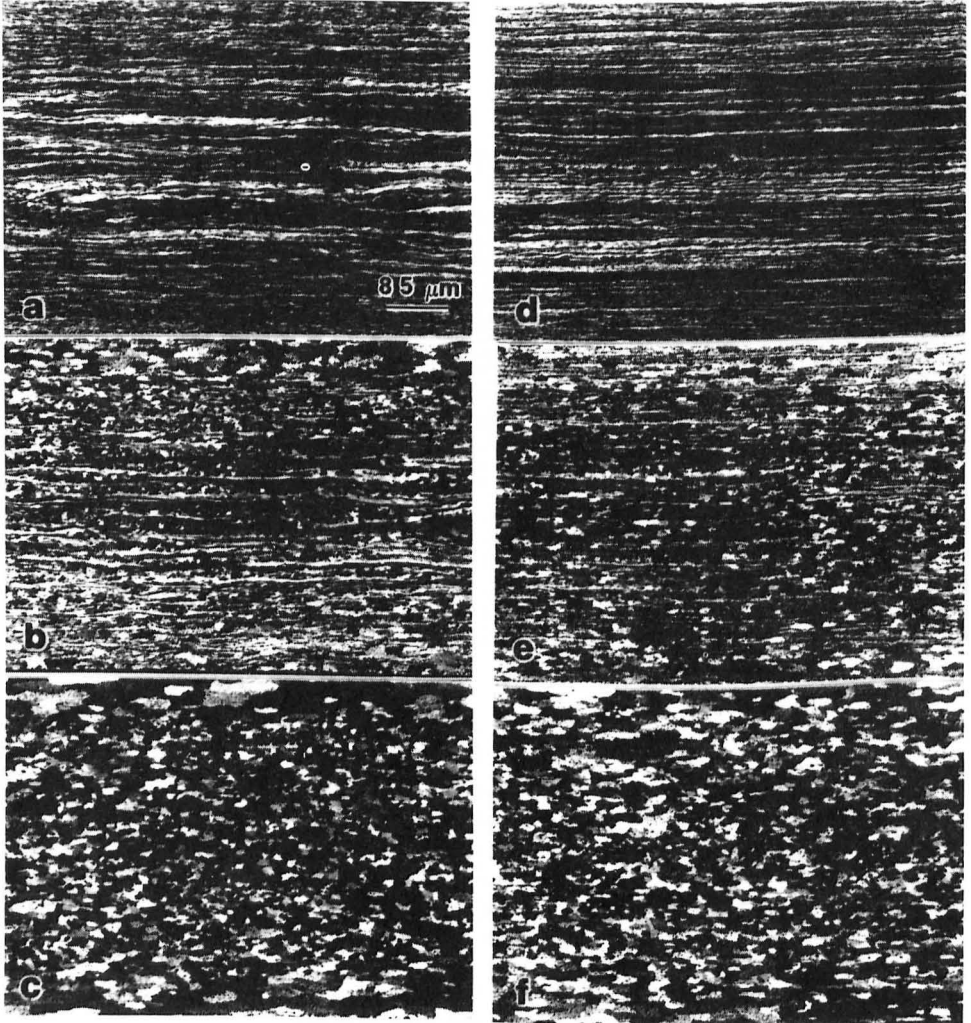


Fig.6. Optical micrographs of anodized strips showing the grain structure: a) #13 as cold rolled, b) #13 heat-treated for 2.5hrs, c) #13 heat-treated for 6.5hrs, d) #7 as cold rolled, e) #7 heat-treated for 2.5hrs, f) #7 heat-treated for 6.5hrs

After recrystallization, Fig. 6c,f, negligible difference in grain structure are found between the two strips, large grains near the surface are characteristic for both. Hardness measurements with low load (100g) were performed at the surface region and in the halfway between the surface and centre, presented in Table II as relative values.

Strip/Heat Treatment	Surface	1/4t
#7/ 0hrs	2.07	1.91
#13/ 0hrs	1.88	1.65
#7/ 6.5hrs	1.21	1
#13/ 6.5hrs	1.1	1.08

Table II. Relative hardness measurements near the surface and at 1/4 thickness.

A $\{112\}\langle 111\rangle$ cold rolled texture was found for both specimens, most pronounced for strip #7 near the surface, Fig. 9. During recrystallization a cube texture is established, strongest near the surface and less sharp towards the centre.

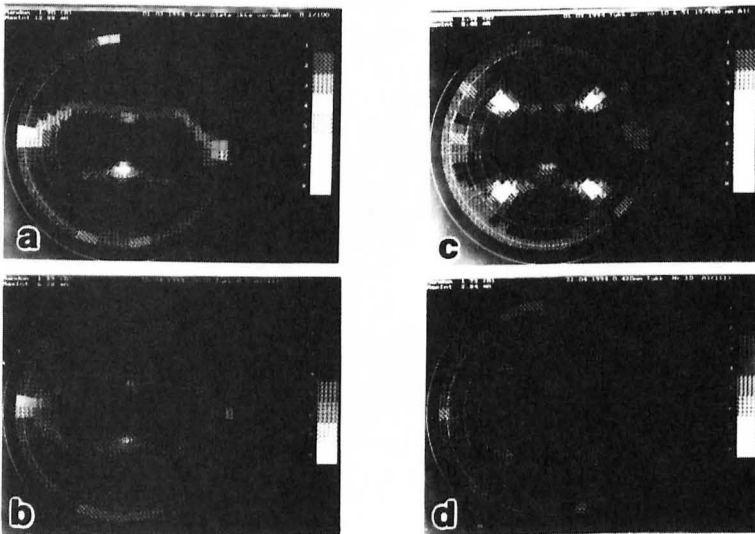


Fig.7. (111) pole figures from strip #7: a) surface as cold rolled, b) 1/4t as cold rolled, c) surface as recrystallized, d) 1/4t as recrystallized

A further study of size and orientations of grains and subgrains were carried out in TEM which was used also for identification of secondary particles. Grains corresponding to the deformation texture are seen in Fig. 8; the Moire pattern in the inset indicate a subgrain size of 100nm. Fig. 9 show a partly recrystallized structure formed after 2.5hrs heat treatment: 1 is a large grain with cube orientation, grain 2 and 3 are much smaller with $\{110\}\langle 100\rangle$ and $\{103\}\langle 100\rangle$ orientation respectively. The TEM micrographs revealed considerable variation in the secondary particle distribution across the strip, Fig. 10. A large number of particles around 50 nm in diameter is seen near the surface, most clearly after 3hrs heat treatment. From electron diffraction patterns they were identified as Al_6Fe .

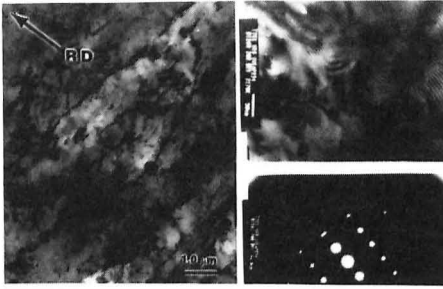


Fig.8. Low magnification TEM micrograph from #7 as cold rolled. Diffraction inset: $\{112\}\langle 111\rangle$ orientation.

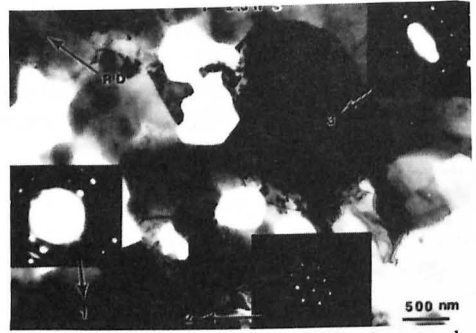


Fig.9. Low magnification TEM micrograph from the surface region of #7, heat-treated 2.5hrs.

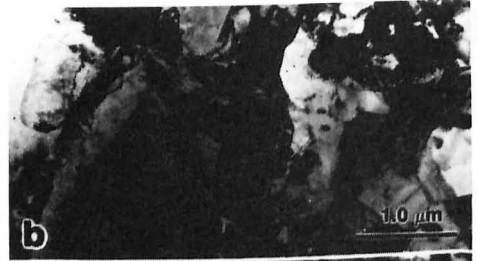


Fig.10. Low magnification TEM micrographs showing the microstructure from strip #7: a) surface, 2.5hrs heat-treatment, b) near centre, 2.5hrs heat-treatment, c) surface 3.0hrs heat-treatment, d) near centre, 3.0hrs heat-treatment.

Discussion

By optical characterization of the as-cast microstructure, cooling rates across the strip are quantified and solidification front can be located. These observations can be compared with results of computer modelling of the temperature and material flow. The present study show a marked difference in the cast structure between the 5mm and the 1.9mm strip. The dual structure found within the grains of the coarser strip, viz. a coarse equiaxed dendritic area joined with another area with a cell structure characteristic of unidirectional solidification, can be explained by nucleation in the two phase mushy zone. The nucleated grains will grow slowly until they establish contact with the solidification front, wherupon heat extraction through the solid increases considerably - resulting in a marked change in the growth pattern.

The volume fraction of the dendritic area is equal to the fraction solid at the time directional solidification starts. In the 1.9mm strip a different grain structure is formed. No cell structure is seen in the grains, which contain an equiaxed structure only, and are smaller compared with the thicker strip. The observations suggest that the cooling rates are lower during casting of the thinner strip, presumably with a deeper mushy zone. The slower cooling rate is confirmed also by DAS measurements, which indeed indicate a longer solidification time for the 1.9mm strip. This somewhat unexpected decrease in cooling rate with reduced thickness must be seen in relation to the higher productivity.

Microstructure differences between the thin and thick strips and between different levels in the strip were found also after the recrystallization treatment. Sharp textures and large grains appear near the surface of the cold rolled and annealed strips. $\{100\}\langle 010\rangle$ and $\{103\}\langle 010\rangle$ are common grain orientations seen in TEM. The texture maps taken halfway between the surface and the centre may indicate contributions of other texture components, possibly $\{112\}\langle 111\rangle$, i.e. parallel to the rolling texture. The differences in the recrystallized grain size and textures may be related to the distribution of primary particles, which are less abundant near the surface. Here the cooling rate is higher and a large number of secondary particles, mostly Al_6Fe were found after annealing. The dispersoids may affect the recovery and recrystallization behaviour in a profound way, by stabilizing a subgrain network [12]. This appears as a likely explanation for the higher hardness found in the surface area after recrystallization, despite the larger grain size in the region.

Acknowledgements

Our thanks to Hydro Aluminium for the samples and financial support. Research Fellowships from The Research Council of Norway for two of us (V.H and B.S.B) are gratefully acknowledged. We are also indebted to T.L.Rolfen and others at SINTEF Oslo for collections of texture maps and discussions. Thanks also to P.T.Zagierski for optical micrographs.

References

1. A. Mo, S.H. Høydal, Proceeding from Modeling of Casting, welding and advanced solidification processes VI, Palm Coast Florida, March 21-26, 1993
2. B.C. Oberländer, Internal report SINTEF Oslo, no 860131-1, 1987 (in norwegian)
3. C. Simensen et al., Fresenius Z. Anal. Chem., **319**, p286, 1984
4. H. Matyja et.al., J. Inst. Metals, **96**, 30, 1968
5. I. Miki et.al., J. Japan Inst. Light Metals, **25**, 1, 1975
6. L. Bäckerud et.al., Solidification Characteristics of Aluminium Alloys, Universitetsforlaget, Oslo, 1986
7. J. Strid, privat communications
8. P. Skjerpe, Acta Cryst., **B44**, p480, 1988
9. D.A. Porter, H. Westengen, Quantitative Microanalysis with High Spacial Resolution, p94, London: The Metal Society, 1981
10. H. Westengen, Z. Metallkd., **73**(6), p360, 1982
11. P. Skjerpe, Metall. Trans., **18A**, p189, 1987
12. Y. F. Cheng et.al., Proceedings from ICAA3, volume II, p50, Trondheim, June 1992